

The Value of Enhanced Three-dimensional Brain volume magnetic Resonance Imaging in tolosa-hunt Syndrome: A Clinical Retrospective Study

Guoliang Lin

Wenzhou Medical University Second Affiliated Hospital

Shushu Zhang

Wenzhou Dongfang Vocational and Technical Collage

Beilei Hu

Wenzhou Medical University Second Affiliated Hospital

Songfang Chen

Wenzhou Medical University Second Affiliated Hospital

Ming Zou

Wenzhou Medical University Second Affiliated Hospital

Yuqiang Gong

Wenzhou Medical University Second Affiliated Hospital

Bihuan Cheng

Wenzhou Medical University Second Affiliated Hospital

Zhiyong He (✉ wyyey0755@163.com)

Wenzhou Medical University Second Affiliated Hospital <https://orcid.org/0000-0003-0631-2470>

Research article

Keywords: THS, MRI, 3D-BRAVO, Headache

Posted Date: July 6th, 2020

DOI: <https://doi.org/10.21203/rs.3.rs-39332/v1>

License:   This work is licensed under a Creative Commons Attribution 4.0 International License.

[Read Full License](#)

Abstract

Background: The study aimed to evaluate the enhanced three-dimensional brain volume magnetic resonance imaging (3D-BRAVO) in the diagnosis of Tolosa-Hunt syndrome (THS). **Methods:** we described 21 patients with THS and their case records including clinical syndromes and neuroradiologic features by conventional MRI and enhanced 3D-BRAVO. **Results:** 19 patients showed enhancement in the cavernous sinus through 3D-BRAVO. 16/19 had ipsilateral enhanced lesions involved 4-10 continuous slices in cavernous sinus on 3D-BRAVO scan. Both local size enlargements and enhancement in the cavernous sinus were found in 3 patients. The rest 2 patients performed negative results on neither conventional MRI nor enhanced 3D-BRAVO. **Conclusions:** enhanced 3D-BRAVO imaging demonstrated a high detection rate in the cavernous sinus, which may promote our understanding of Tolosa-Hunt syndrome.

Introduction

Tolosa-Hunt syndrome (THS) was a rare disease characterized by painful ophthalmoplegia, which originally described by Dr. Eduardo Tolosa. Pathologic changes were not only in the region of cavernous sinus but also penetrating cranial nerves III, IV, VI, as well as the superior division of the fifth cranial nerve, added by Hunt and his colleagues. It was identified that as a benign inflammatory process in the region of cavernous sinus by biopsy and well respond to corticosteroids.[1–3] Prior studies frequently disclosed enlargement and asymmetric enhanced lesion in the region of the cavernous sinus, especially in the coronal view, and it was assumed the pathology to be granulomatous through magnetic resonance image (MRI) or computed tomography (CT).[4, 5] As radiologic technology advanced, particularly high resolution MR made it possible to study the region of the cavernous sinus. Recently, the International Classification of Headache Disorders-3 (ICHD-3) criteria for THS suggested that MRI played an important role in demonstrating granulomatous lesions and ruling out other causes of painful ophthalmoplegia like nasopharyngeal carcinoma, sphenoid sinusitis, pituitary adenoma, vasculitis, meningitis, sarcoidosis or diabetes mellitus.[5] Despite its ability to identify THS as an inflammatory disease, non-enhanced MRI findings may also make mistakes or perform negative results.[6] Guedes and Akpinar demonstrated cavernous sinus enhancement using a slice thickness of 3 mm through fat suppression pattern.[7] [8] Researchers were likely achieved method to reduce “false-negative” through enhanced MRI with fat suppression, but most of these were case reports. There was lack of series or multiple cohorts’ studies to improve sensitivity to identify pathological changes in cavernous sinus. Thus, a better protocol for visualization of cavernous sinus should be put on the agenda. Here we studied clinical charts and neuroradiological images of patients with THS, clued to the differentiation between distinct etiologies of cavernous sinus and tried to improve the diagnostic accuracy of THS through systemically evaluating radiological approach, which may help in differentiating cavernous sinus disease.

Patients And Methods

All of 30 patients suspected with THS were consecutively enrolled from the neurology department and

Loading [MathJax]/jax/output/CommonHTML/jax.js ated Hospital and Yuying Children’s Hospital of Wenzhou

Medical University, China, from 2016 to 2019. Informed consent to participate in the study was obtained from all patients or their families, and the study was approved by the Ethics Committee of the Second Affiliated Hospital and Yuying Children's Hospital of Wenzhou Medical University. All patients were evaluated by neurologists according to the International Classification of Headache Disorders criteria II for Tolosa-Hunt syndrome. Clinical features and neuroradiologic characterizes presented in all patients were reviewed. All patients were required to get CT scans, non-enhanced and enhanced 3D-BRAVO MRI examinations, but 9 patients refused to accept enhanced 3D-BRAVO MRI.

Brain MRI scans in all patients were performed using 3.0-T GE Signa HDxt clinical MR system (General Electric, Milwaukee, WI, USA). T1 weight-image(WI) (TR = 1889 ms; TE = 785 ms; FA = 90°; field of view = 240 × 240 mm²; matrix size = 384*224), T2 WI sequence(TR = 4480 ms; TE = 117 ms; FA = 90°; field of view = 240 × 240mm²; matrix size = 384*224), T2-WI flair-sequence(TR = 7157 ms; TE = 168 ms; FA = 90°; field of view = 240 × 240 mm²; matrix size = 288*160), enhanced brain volume image(3D-BRAVO, gadolinium-DTPA 0.1 mL/kg weight, TR = 8 ms; TE = 3 ms; FA = 90°; field of view = 240 × 240 mm²; matrix size = 256*256,SL = 1.2 mm, sp = 0.6 mm) should be needed. 2D enhanced images were reconstructed from the 3D datasets by a research MR radiographer (TR = 8 ms; TE = 3 ms; FA = 15°; field of view = 240 × 240 mm²; matrix size = 256*256; SL = 4.75 mm). All images from patients were identified by an experienced neuroradiologist and an experienced neurologist. A Philips Brilliance CT machine was used for brain angiography to exclude encephalorrhagia, aneurysms, metastases, and pituitary masses when hospital arrival.

Results

Clinical features

13 males and 8 females were included (age range from 18–73 years). Diplopia was found in 12 patients and ptosis in 11 patients. 10 patients experienced orbital pain on the right side, 4 experienced orbital pain on the left side, 5 and 1 were suffered from forehead pain on the left side and right side, respectively. 1 patient had a headache on both sides of his forehead. Abnormal abduction was found in 2 patients. All clinical findings were summarized in Table 1.

Neuroradiologic features

All patients had CT angiography, but nothing was found. 3 out of 21 (1 was on the right side, the others two were on the left side) presented asymmetrically localized enlargement of cavernous sinus on non-enhanced MRI. 19 of these 21 patients showed enhanced lesions in the cavernous sinus through enhanced 3D-BRAVO scans. 16/19 had ipsilateral enhanced imaging involved 4–10 continue slices in cavernous sinus on 3D images (Fig. 1). Cavernous sinus homogeneous enhancement was found in 9 patients (Fig. 2a). 3 of these 16 demonstrated orbital apex cord-like enhancement. 3 presented cavernous sinus homogeneous and orbital apex cord-like enhancement. 1 of the 16 performed orbital apex homogeneous enhancement (Fig. 2c). Enlargement and dural enhancement in both sides of the area of

cavernous sinus were found in 1 of these 3. Thickening and continuity of the dural contour were presented in all of these 19 instances on enhanced 3D-BRAVO. 2 patients demonstrated negative results both on non-enhanced and enhanced MR scans. In order to further observation, we reconstructed our 3DBROVA to 2D image. 13 patients, in the coronal view, were disclosed enhanced signal only involved in one to two slices on 2D-reconstructed images. 6 patients had negative results when their images were reconstructed (Fig. 2b, 2d).

Discussion

Since the early description in 1966, numerous reports suggested THS accompanied by unilateral orbital pain or periorbital headache, which can be described as sharp, burning, server instance, with three cranial nerve palsy, including III, IV, or VI cranial nerves.[9] In our study, all of our patients presented the third cranial nerve impairment, this is the same as Arcaya's study, and similar to Hao's report (91%). And all patients had headaches or orbital pain, which suggested the involvement of the first division of the fifth cranial nerve, but no research had discussed before. It had been reported that 60–70% of cases of THS experienced the sixth cranial nerve paresis[10]. But it was only 9% disclosed in our study.

Granulomatous inflammation demonstrated on MRI or biopsy had been highlighted in the latest criteria. [6] Nevertheless, Mullen noted this may lead to false-negative and false-positive results. They reported 10 patients who were concerning as THS, but with high false-negative (40–57%) due to unremarkable non-enhanced MRI.[11] In our study, nearly 86% (19/21) were negative on their non-enhanced MRI. It seemed insufficient to show granulomatous inflammation on non-enhanced MRI.

Given the high false-negative rate of non-enhanced MRI, researchers had to look for an efficacious method to improve the sensibility of diagnosis. Studies suggested thin the slice thickness and enhanced MRI with fat suppression maybe another option.[12] An observation by applying high resolution MR sequences (slice thickness = 2.5-3 mm), from Schuknecht and his colleagues, displayed 75% pathologic finding.[13] Hao gave post-contrast fat suppression MRI scans to the “non-enhanced MRI negative” patients. Abnormalities on post-contrast fat suppression MRI were observed in the cavernous sinus and orbital apex in these patients. They supposed such patients may in the early period of THS which lesions can't be detected on non-enhanced MRI. Although it seemed evidence that fat suppression increased the detection ability, Abdelghany presented a case of THS accompanied by an unremarkable lesion through the same neuro-image method, suggested a new inflammatory signal may be found after follow-up enhanced MRI.[14]

As we know, it was the first time for us to use an enhanced 3D-BRAVO scan in THS. We found 90% of our patients show enhanced signal involved in 4–10 continuous slices, while there were negative on their non-enhanced MRI. According to our reconstructed data, 61% (13/21) patients showed enhancement involved in one to two slices, but it seemed difficult for us to make a diagnosis based on such condition. Additionally, our CTA results didn't show any lesions where there were positive results on our 3D data. Thus, we supposed that the size of the lesion in the cavernous sinus was too small to be detected on non-

enhanced MRI but could be observed on enhanced 3D-BROVA MRI. This met the idea that thin the slice thickness may play a diagnostic role in THS.[12]

However, a pathological sample diagnosis from one patient who was suspected as THS triggered us to reconsider our study. We noted that a hyperintense signal showed in the area of the orbital apex on 3D-BROVA MRI and was diagnosed with granulomatous inflammation by two senior neuroradiologic specialists, while Schwannoma of the oculomotor nerve was her biopsy diagnosis. This case was likely to remind us that magnetic resonance can only be used as an auxiliary tool for diagnosis, but not for making a definite diagnosis. The application of the criteria-3 produced more often false-positive and false-negative diagnoses.[11]

Conclusion:

THS was a benign neurologic disease that was caused by nonspecific granulomatous inflammation in the cavernous sinus. MRI had facilitated us to exclude other reasons for painful ophthalmoplegia. Enhanced 3D-BROVA imaging showed more finely to demonstrate the cavernous sinus and promote our understanding of THS.

Abbreviations:

THS = Tolosa-Hunt syndrome, MRI = magnetic resonance imaging, 3D-BRAVO = three-dimensional brain volume magnetic resonance imaging, CT = computed tomography.

Declarations

Ethics approval and consent to participate: Informed consent to participate in the study was obtained from all patients or their families, and the study was approved by the Ethics Committee of the Second Affiliated Hospital and Yuying Children's Hospital of Wenzhou Medical University.

Consent for publication: Written informed consent for publication was obtained from all participants.

Availability of data and material: All data generated during this study are included in this published article.

Competing of interest: None.

Funding: None.

Authors' contributions: Zhiyong He, the corresponding author, contributed to conceive and design the study, interpret the data. Beilei Hu, Songfang Chen, Ming Zou, Yuqiang Gong and Bihuan Cheng contributed to the cases collection in this study. Guoliang Lin and Shushu Zhang contributed to perform the data and write the paper. All authors have given approval to the final version of the

Acknowledgements: The research received no grant from any funding agency.

References

1. Tolosa E (1954) Periarteritic lesions of the carotid siphon with the clinical features of a carotid infraclinoidal aneurysm. *J Neurol Neurosurg Psychiatry* 17(4):300–302
2. Kline LB, Hoyt WF (2001) The Tolosa-Hunt syndrome. *J Neurol Neurosurg Psychiatry* 71(5):577–582
3. Hunt WE, Meagher JN, Lefever HE, Zeman W (1961) Painful ophthalmoplegia. Its relation to indolent inflammation of the cavernous sinus. *Neurology* 11:56–62
4. de Arcaya AA, Cerezal L, Canga A, Polo JM, Berciano J, Pascual J (1999) Neuroimaging diagnosis of Tolosa-Hunt syndrome: MRI contribution. *Headache* 39(5):321–325
5. Amrutkar C, Burton EV, Tolosa-Hunt Syndrome, StatPearls, Treasure Island. (FL), 2020
6. Lueck CJ (2018) Time to retire the Tolosa-Hunt syndrome? *Pract Neurol* 18(5):350–351
7. Guedes BV, da Rocha AJ, Zuppani HB, da Silva CJ, Sanvito WL (2010) A case review of the MRI features in alternating Tolosa-Hunt syndrome. *Cephalalgia* 30(9):1133–1136
8. Akpinar CK, Ozbenli T, Dogru H, Incesu L (2017) Tolosa-Hunt Syndrome - Cranial Neuroimaging Findings. *Noro Psikiyatrs Ars* 54(3):251–254
9. Iaconetta G, Stella L, Esposito M, Cappabianca P (2005) Tolosa-Hunt syndrome. extending in the cerebello-pontine angle. *Cephalalgia* 25(9):746–750
10. Tessitore E, Tessitore A (2000) Tolosa-Hunt syndrome preceded by facial palsy. *Headache* 40(5):393–396
11. Mullen E, Rutland JW, Green MW, Bederson J, Shrivastava R (2020) Reappraising the Tolosa-Hunt Syndrome Diagnostic Criteria: A Case Series. *Headache* 60(1):259–264
12. Hao R, He Y, Zhang H, Zhang W, Li X, Ke Y (2015) The evaluation of ICHD-3. beta diagnostic criteria for Tolosa-Hunt syndrome: a study of 22 cases of Tolosa-Hunt syndrome. *Neurol Sci* 36(6):899–905
13. Schuknecht B, Sturm V, Huisman TA, Landau K (2009) Tolosa-Hunt syndrome: MR imaging features in 15 patients with 20 episodes of painful ophthalmoplegia. *Eur J Radiol* 69(3):445–453
14. Abdelghany M, Orozco D, Fink W, Begley C (2015) Probable Tolosa-Hunt. syndrome with a normal MRI. *Cephalalgia* 35(5):449–452

Tables

Table 1. The clinical features of patients with THS

Patients	Age, y	Sex	Affected side	Paresis Cranial nervous	Enhanced image	
					3D-BRAVO	Coronal view on 2D-reconstructed
1	58	M	L	III, V	Dural contour homogeneous enhanced	Enlargement and asymmetric enhanced
2	69	F	L	III, V, VI	Dural contour homogeneous enhanced	Enlargement and asymmetric enhanced
3	54	F	R	III, V	Orbital apex cord-like enhanced, dural contour homogeneous enhanced	Enlargement and asymmetric enhanced
4	31	M	R	III, V	Orbital apex cord-like enhanced	Enlargement and asymmetric enhanced
5	48	M	R	III, V, VI	Dural contour homogeneous enhanced	Enlargement and asymmetric enhanced
6	22	M	R	III, V	Orbital apex homogeneous enhanced	No enhanced
7	41	M	L	III, V	Dural contour homogeneous enhanced	No enhanced
8	58	M	L	III, V	Dural contour homogeneous enhanced	No enhanced
9	46	M	R	III, V	Dural contour homogeneous enhanced	Enlargement and asymmetric enhanced
10	56	M	L	III, V	Dural contour homogeneous enhanced	No enhanced
11	73	F	R	III, V	Dural contour homogeneous enhanced	No enhanced

Patients	Age, y	Sex	Affected side	Paresis Cranial nervous	Enhanced image	
					3D-BRAVO	Coronal view on 2D-reconstructed
12	71	F	L	III, V	Dural contour homogeneous enhanced	Enlargement and asymmetric enhanced
13	69	F	R	III, V	Dural contour homogeneous enhanced	Enlargement and asymmetric enhanced
14	49	M	L	III, V	Dural contour homogeneous enhanced	Enlargement and asymmetric enhanced
15	62	F	R	III, V	Dural contour homogeneous enhanced	No enhanced
16	54	M	R	III, V	NO	NO
17	62	M	R	III, V	NO	NO
18	68	M	L/R	III, V	Both sides of dural contour homogeneous enhanced	Enlargement and asymmetric enhanced
19	18	F	L	III, V	Dural contour homogeneous enhanced	Enlargement and asymmetric enhanced
20	62	M	L	III, V	Dural contour homogeneous enhanced	Enlargement and asymmetric enhanced
21	37	F	L	III, V	Orbital apex cord-like enhanced	Enlargement and asymmetric enhanced

Figures

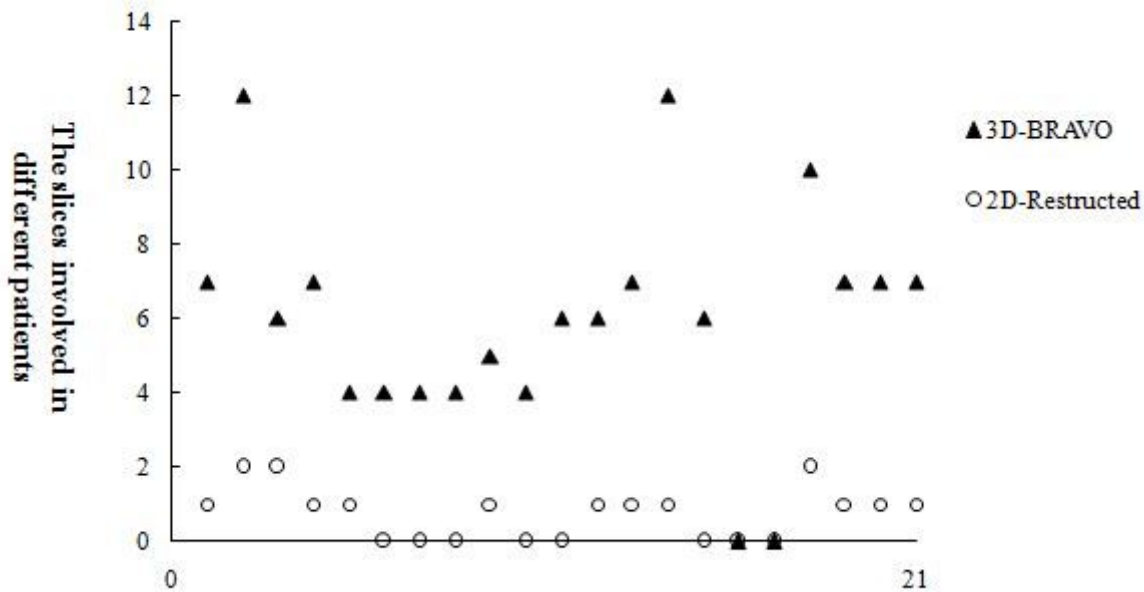


Figure 1

Loading [MathJax]/jax/output/CommonHTML/jax.js

Figure 1. Slices involved in 21 patients. Different slices involved in 21 patients on 3d-bravo MRI (black triangle) and its corresponding hollow circle represent slices involved in 2d-restructured data.

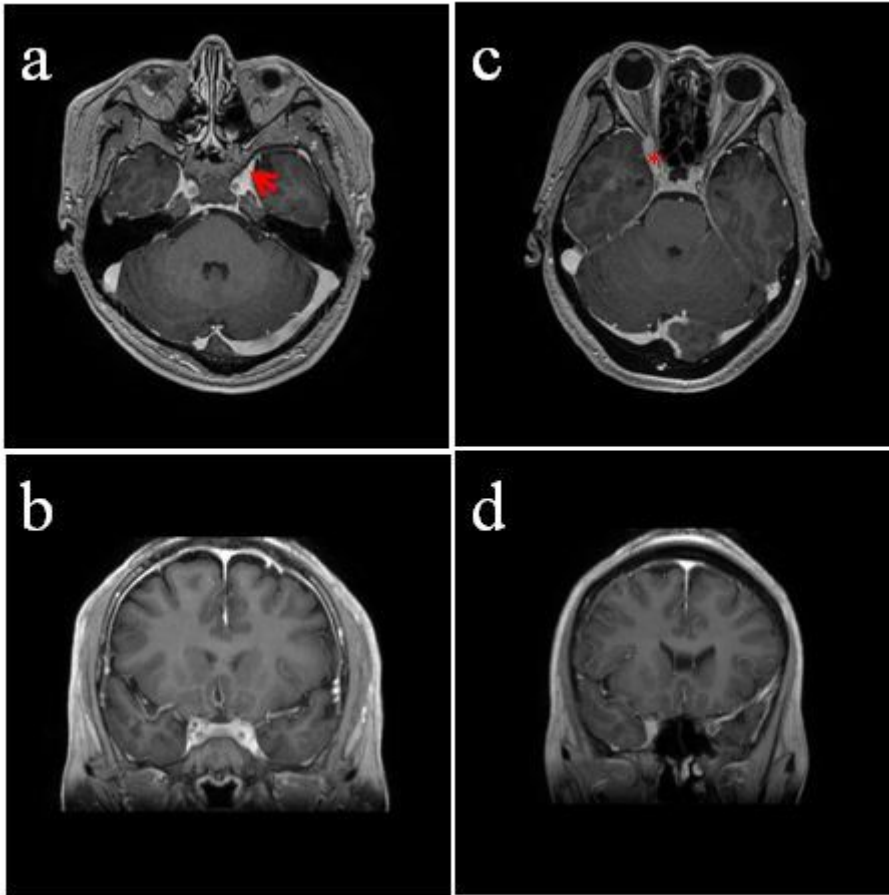


Figure 2

Figure 2. Lesions demonstrate on enhanced 3d-bravo and 2d-reconstructed images. (a) Left side cavernous sinus homogeneous enhancement (red arrow) and (b) left side cavernous sinus lesion show on the coronal view on 2d -reconstructed images. (c) Right side orbital apex homogeneous enhancement (red asterisk) on 3d-bravo image. (d) Right side side orbital apex enhancement show on the coronal view on 2d -reconstructed images.